Dense carrier gas effect in vapor phase nucleation

Vladimir M. Novikov*
Physics Department, California Institute of Technology, Pasadena, California 91125

Oleg V. Vasil'ev† and Howard Reiss
Department of Chemistry and Biochemistry, University of California, Los Angeles, 405 Hilgard Avenue, Los Angeles, California 90095
(Received 17 January 1997)

By simple Monte Carlo simulation it is demonstrated that the capture of vapor molecules by a drop is affected by a dense background gas far from the Knudsen regime, and deep within the free molecule regime. The corresponding effect on steady-state nucleation is considered. For several representative examples the slopes of critical supersaturation vs carrier gas pressure are obtained and compared with experimental data. [S1063-651X(97)04805-8]

PACS number(s): 64.60.Qb, 64.70.Fx, 51.10.+y

I. INTRODUCTION

Recently, the theory of the capture of vapor molecules by a drop was revised for drop sizes important in vapor to liquid nucleation [1,2]. The revision is due to the drop's attractive potential, and for simple potentials the enhancement of the capture rate was obtained analytically. The revised theory opens the possibility of carrier (background, non-nucleating) gas influence on the nucleation rate, because the enhancement is affected by the carrier gas, and this effect is repeated many times during the drop's growth to critical size [1]. In the present work we have observed the carrier gas effect by means of simulation. We present the simulation results for drops of subcritical, critical, and, to some extent, above critical sizes, and calculate the resulting multiplicative effect of the carrier gas on the nucleation rate. The resulting effect is compared with experimental data [3].

II. STEADY-STATE NUCLEATION

The steady-state rate of nucleation is given by [1,4]

$$J=\rho\left(\sum_{j=1}^{\infty}\frac{1}{\gamma(j+1)}\prod_{l=1}^{j}\frac{\gamma(l+1)}{\beta(l,c)}\right)^{-1}, \tag{1}$$

where ρ is the number density of vapor molecules, c is the carrier gas pressure, $\beta(j,c)$ is the rate at which vapor molecules are absorbed in a drop of j molecules, and $\gamma(j)$ is the rate at which molecules evaporate from the drop. The evaporation rate $\gamma(j)$ is far less sensitive to the carrier gas density than the impingement rate $\beta(j,c)$, and it is assumed that $\gamma(j,c)=\gamma(j)$. We discuss and justify this assumption in Sec. IV.

We introduce the carrier gas factor $\xi(j,c)=\beta(j,c)/\beta(j,0)$, the function $A(j,c)=\Pi_{l=1}^{j}\xi^{-1}(l,c)$, the function $\chi(j)=\Pi_{l=1}^{j-1}\gamma(l+1)/\beta_e(l)$, $\chi(1)=1$, and the conventional supersaturation ratio $S=\beta(j,0)/\beta_e(j)$, where $\beta_e(j)\equiv\beta_e(j,0)$ is the impingement rate at equilibrium (the vapor is saturated) and without the carrier gas. Then

$$\frac{\rho}{J}=\sum_{j=1}^{\infty}\frac{\chi(j)A(j,c)}{\beta_e(j)S^j}. \tag{2}$$

The critical supersaturation $S_{\rm cr}(c)$ is defined by the equation

$$\frac{\rho}{J_0}=\sum_{j=1}^{\infty}\frac{\chi(j)A(j,c)}{\beta_e(j)S_{\rm cr}^j(c)}, \tag{3}$$

where $J_0=1/\mathrm{cm}^3$ sec. Differentiating this equation with respect to c, we obtain

$$\partial_c S_{\rm cr}(c)=\frac{\displaystyle\sum_{j=1}^{\infty}\frac{\chi(j)\partial_c A(j,c)}{\beta_e(j)S_{\rm cr}^j(c)}}{\displaystyle\sum_{j=1}^{\infty}\frac{\chi(j)jA(j,c)}{\beta_e(j)S_{\rm cr}^{j+1}(c)}}. \tag{4}$$

In the capillarity approximation

$$\chi(j)=\exp\left(\frac{(36\pi)^{1/3}\varrho(jV)^{2/3}}{kT}\right),\quad j>1, \tag{5}$$

where ϱ is the bulk surface tension, V is the volume per molecule in the liquid coexisting with the vapor, T is the temperature, and k is the Boltzmann constant [4,5]. The impingement rate

$$\beta_e(j)=\eta(j)\beta_e^0(j)=\eta(j)\left(\frac{162}{\pi}\right)^{1/6}\sqrt{kT/m}\,\rho_e(jV)^{2/3}, \tag{6}$$

where m is the mass of the vapor molecule, ρ_e is the number density of saturated vapor molecules, and $\eta(j)$ is the enhancement factor, which corrects the conventional expression $\beta_e^0(j)$ for the interaction between a drop and a vapor molecule [1,2]. This interaction is approximated by the potential [2]

$$U(j,r)=-\frac{j\alpha}{[r^2-R_0^2(j)]^3}, \tag{7}$$

*Permanent address: Institute for Nuclear Research, 60th October Anniversary Prosp., 7a, 117312 Moscow, Russia.

†Present address: Department of Chemical Engineering, University of California, Los Angeles, Los Angeles, CA 90095-1592.

where $R_0(j)=[(3/4\pi)jV]^{1/3}-a/2$, a is the vapor molecule diameter and the parameter α corresponds to the tail of the attractive potential $-\alpha/r^6$ between vapor molecules. A vapor molecule that reaches the distance R_0+a is counted as captured by the drop.

For the potential (7) the enhancement factor is given by [2]

$$\eta(j)=1+\int_1^{+\infty}dy\left[1-\left(1+\frac{\mu(j)}{h(\nu(j)y)}\right)\exp\left(-\frac{\mu(j)}{h(\nu(j)y)}\right)\right], \tag{8}$$

where

$$\mu(j)=\frac{27\alpha j}{kTR_0^6(j)}, \tag{9}$$

$$h(z)=2z^3-9z^2+108z+27+(2z^2-12z-54)\sqrt{z^2+3z}, \tag{10}$$

$$\nu(j)=\left(1+\frac{a}{R_0(j)}\right)^2. \tag{11}$$

(The variables μ and ν here correspond to μ/ν^3 and ν^{-1} of [2].)

If the interaction between vapor molecules is approximated by the Lennard-Jones potential

$$u_v(r)=4k\epsilon_v\left[\left(\frac{\sigma_v}{r}\right)^{12}-\left(\frac{\sigma_v}{r}\right)^{6}\right], \tag{12}$$

then $a=2^{1/6}\sigma_v$ and $\alpha=4k\epsilon_v\sigma_v^6$ [6,7].

The enhancement is affected by a dense carrier gas; this effect is reflected in the carrier gas factor $\xi(j,c)<1$ [1]. The slope of the critical supersaturation $S_{\rm cr}$ vs c, Eq. (4), comes from the following dependence of $A(j,c)$ on c:

$$\partial_c A(j,c)=-A(j,c)\sum_{l=1}^{j}\frac{\partial_c\xi(l,c)}{\xi(l,c)}>0. \tag{13}$$

III. CARRIER GAS EFFECT

There has been considerable interest in the Knudsen transition regime, for drops of size comparable to the molecular mean free path in the vapor [8–10]. The Knudsen regime separates the limiting behaviors of small drops (free molecule regime) from those of larger drops (hydrodynamic regime) [11] (see also references in [10]). It is interesting that at the opposite edge of the free molecule regime, for very small drops, there is another transition regime, of similar nature, such that an extremely dense carrier gas should recover the conventional impingement rate $\beta_e^0(j)$, by suppressing the enhancement [1]. Qualitatively, this regime is expected under conditions such that the drop size is comparable to the average vapor or carrier gas intermolecular distance. Quantitatively, however, the problem is more difficult than that for the Knudsen regime. In the Knudsen regime the trajectories of vapor molecules towards the drop can be treated as straight lines, and the encounters with other vapor molecules [9] or with carrier gas molecules [10] can be regarded as local collisions. In the new transition regime the trajectories of the vapor molecules towards the drop are curved due to the drop's attractive potential, and encounters with vapor or carrier gas molecules are small angle deflections of these trajectories due to the intermolecular interaction [1]. This renders the problem of analytical study difficult and suggests simulation. In the present work we have observed the carrier gas effect and the tail of the associated transition regime by means of a simple specially designed simulation.

The interaction between a drop and a vapor molecule is approximated by the potential $U(j,r)$, Eq. (7). A vapor molecule is shot from the sphere of radius $R_s=3(R_0+a)$ centered at the origin. The initial velocity $\mathbf{v}$ of the molecule is simulated from the distribution

$$f(\mathbf{v})\sim v\,\omega(v), \tag{14}$$

where $\omega(v)\sim\exp(-mv^2/2kT)$ is the Maxwell distribution. (But only the directions towards the interior of the sphere are selected.) The movement of the molecule is simulated as described below until it reaches the sphere of radius R_0+a centered at the origin (successful trajectory, the drop is reached) or the sphere of radius R_s (unsuccessful trajectory).

This movement is calculated, using discretized Newton equations with a time step Δt. Each step is accepted with a probability $(1-\phi)$, where ϕ is the probability of interaction with a carrier molecule:

$$\begin{aligned}\phi&=\pi r_{\rm cut}^2\rho_c\Delta t\int d\mathbf{v}_c\omega_c(v_c)|\mathbf{v}_c-\mathbf{v}(t)|\\&=\pi r_{\rm cut}^2\rho_c\Delta t\sqrt{2kT/m_c}\left[\left(q(t)+\frac{1}{2q(t)}\right)\mathrm{erf}(q(t))-\frac{\exp[-q^2(t)]}{\sqrt{\pi}}\right],\end{aligned} \tag{15}$$

$$q(t)\equiv\sqrt{m_c/2kT}v(t). \tag{16}$$

Here

$$\omega_c(v_c)=\left(\frac{m_c}{2\pi kT}\right)^{3/2}\exp\left(-\frac{m_cv_c^2}{2kT}\right) \tag{17}$$

is the Maxwell distribution for the carrier gas while ρ_c is its molecular number density. $r_{\rm cut}$ is the distance cutoff on the interaction $u(r)$ between a vapor molecule and a carrier gas molecule:

$$u(r)=4k\epsilon\left[\left(\frac{\sigma}{r}\right)^{12}-\left(\frac{\sigma}{r}\right)^{6}\right],\quad r<r_{\rm cut}=2.5\sigma. \tag{18}$$

For small enough time step $\phi\ll1$.

If an interaction takes place, then in the next step a carrier gas molecule appears on the sphere of radius $r_{\rm cut}$ centered at the position $\mathbf{r}(t)$ of the vapor molecule. The velocity of the carrier gas molecule $\mathbf{v}_c$ is simulated from the distribution

$$\omega_c'(\mathbf{v}_c)\sim\omega_c(v_c)|\mathbf{v}_c-\mathbf{v}(t)|. \tag{19}$$

The site of appearance on the sphere is simulated so that the velocity $\mathbf{v}_c$ is pointed towards the interior of the sphere and

the projection of the site on the plane orthogonal to $\mathbf{v}_c$ is randomly distributed within a circle of radius $r_{\rm cut}$ centered at $\mathbf{r}(t)$.

The Newton equations for both the vapor molecule and the carrier gas molecule are then solved using the potentials $U(j,r)$ and $u(r)$ until one of the following things happens: (1) The vapor molecule reaches the droplet (successful trajectory) or the sphere of radius R_s (unsuccessful trajectory). (2) The carrier gas molecule emerges from the sphere of radius $r_{\rm cut}$ centered at $\mathbf{r}(t)$ and disappears. The movement of the vapor molecule alone then continues, with simulation of the interaction with probability ϕ at each time step Δt.

The parameters corresponding to one of the experiments on the background gas effect in nucleation [3] are perfect for demonstration of the new transition regime. The temperature $T=334.2$ K. The carrier gas density varies from $\rho_c=\rho_0$ to $\rho_c=10\rho_0$, where $\rho_0=8.67\times10^{19}$ cm^{-3} corresponds to the pressure $c=4$ bars. The mass m corresponds to 1-propanol while m_c is the mass of the helium atom. $\epsilon_v=576.7$ K and $\sigma_v=4.549$ Å are the Lennard-Jones parameters for 1-propanol [6]. The drop's size $j=75$ was chosen as characteristic [3] in the sense that the classical estimate for the critical nucleus, $j_{\rm cr}\approx(4\pi/3V)(2\varrho V/kT\ln S)^3$, [5] gives $j_{\rm cr}=75$ at a supersaturation $S=2.4$ (1-propanol liquid density $V^{-1}=7.7\times10^{21}$ cm^{-3} [12], and the surface tension $\varrho=20.6$ dyn/cm [13]). The Lennard-Jones parameters ϵ and σ are estimated from the Lorentz-Berthelot rule $\epsilon=\sqrt{\epsilon_v\epsilon_c}$ and $\sigma=(\sigma_v+\sigma_c)/2$ [7], where $\epsilon_c=10.22$ K and $\sigma_c=2.551$ Å are the Lennard-Jones parameters for helium [6]. The time step was chosen as small as $\Delta t=a/v_{\rm av}$, where $v_{\rm av}$ is the average velocity of a vapor molecule. Decreasing the step size further did not change results. We also must notice that the drop-carrier gas interaction is a second-order effect. Substitution of the Boltzmann distribution (instead of the uniform one) for the carrier gas density around the drop has negligible effect on our results.

The results of 2×10^6 ''shots'' without carrier gas ($\rho_c=0$) as well as for each of 20 carrier gas densities ($\rho_c=n\rho_0$, $n=0.5, 1.0, 1.5,\ldots, 10$), both in the presence and absence of the drop potential, are shown on Fig. 1. The data are normalized to the number of successful trajectories without either the carrier gas or the drop potential. So, the ''Potential ON'' data correspond to the fraction $\beta_e(j,c)/\beta_e^0(j,0)$, while the ''Potential OFF'' data correspond to $\beta_e^0(j,c)/\beta_e^0(j,0)$, where the superscript 0 indicates that the drop potential is switched off [$\beta_e^0(j)=\beta_e^0(j,0)$, see Eq. (6)].

Two important features can be observed in the figure. First, the impingement rate $\beta_e(j,c)$ in the presence of the drop potential is clearly higher than the rate $\beta_e^0(j,c)$ in its absence. [The ''Potential ON'' point at zero corresponds to the enhancement $\eta(j)\equiv\beta_e(j,0)/\beta_e^0(j,0)$ and coincides with the analytical result, Eqs. (8)–(11).] Second, this amplification decreases with an increase of carrier gas density. In fact, the first feature provides an opportunity for the second to appear.

It is clearly seen that, when the mean free path is much larger than the drop size the ''standard'' impingement rate $\beta_e^0(j,c)$ is remarkably insensitive to the carrier gas density, while, in contrast, the amplified rate $\beta_e(j,c)$ *is* sensitive.

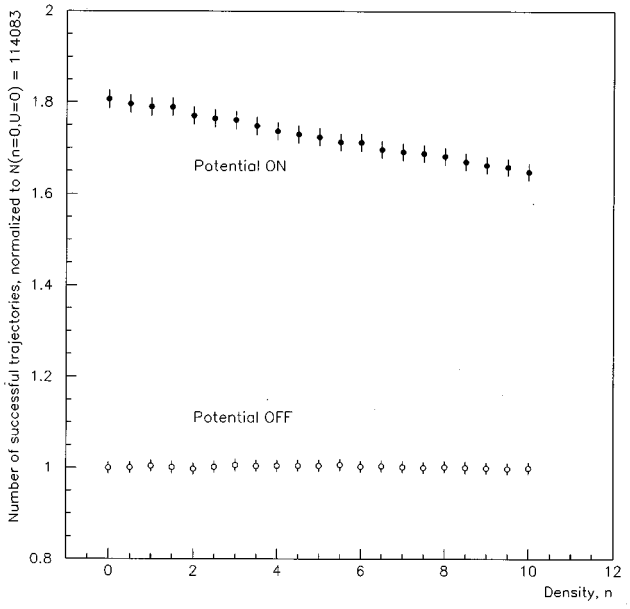

FIG. 1. The number of trajectories ending on the drop, normalized to the one with $n=0$ in the absence of a drop potential. n is the carrier gas density, normalized to $\rho_0=8.67\times10^{19}$ cm^{-3}. The numbers in the presence of the drop potential are denoted by filled circles and, in the absence of a drop potential, by empty circles. The width of the error bars is 3 σ.

This means that small angle deflections due to the carrier gas are able to affect the rate of vapor molecule impingement on the drop, when there is a drop-molecule attraction (typical dispersion force). This occurs when the carrier gas is dense enough to deflect the trajectories of those molecules that reach the drop as a result of the drop's attraction, i.e., the volume per molecule of the carrier gas must be smaller than the volume of the drop. Indeed, the volume of our drop is 75 V, and the value of 75 V ρ_c ranges from 0.85 to 33.78 at $\rho_0<\rho_c<10\rho_0$. Ideally, a further increase in the carrier gas density must eventually cause the ''Potential ON'' data to converge to the ''Potential OFF'' data, so that $\beta_e(j,c)/\beta_e^0(j,c)\to1$, but we could demonstrate this only with ''molecules'' of much smaller radius. Within the physical range of parameters we observe just the tail of the transition from $\eta(j)$ to 1 of $\beta_e(j,c)/\beta_e^0(j,c)$. It is important to realize that while equality of the average carrier gas intermolecular distance and drop's size must correspond to the onset of the transition of $\beta_e(j,c)/\beta_e^0(j,c)$ from $\eta(j)$ to 1, the maximum amplitude of the transition, $[\eta(j)-1]$, is defined by

$$\mu(j)=\frac{A}{j(B-j^{-1/3})^6}, \tag{20}$$

$$\nu(j)=\left(\frac{Bj^{1/3}+1}{Bj^{1/3}-1}\right)^2, \tag{21}$$

where $A=3456\epsilon_v/T$ and $B=(3\sqrt{2}/\pi)^{1/3}\,V^{1/3}/\sigma_v$ [see Eqs. (9) and (11)]. $\eta(j)$ is shown on Fig. 2 for $B=1.2$ and within a reasonable range of j and A. (The values of A and B for the cases considered in Sec. IV are given in Table I).

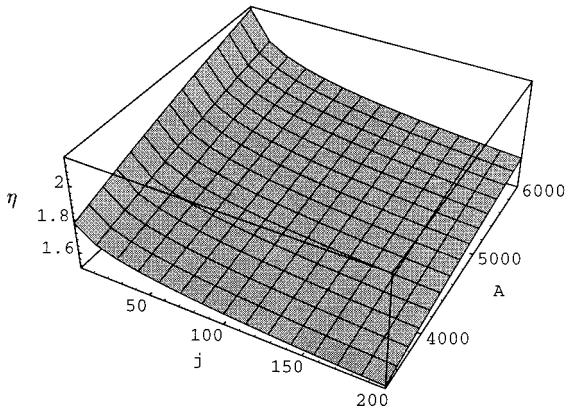

FIG. 2. The enhancement η vs the drop size j and the parameter $A \equiv 3456\epsilon_v/T$ at $B \equiv (3\sqrt{2}/\pi)^{1/3} V^{1/3}/\sigma_v = 1.2$.

Thus, in conclusion, we have shown by simple simulation that the rate of capture of vapor molecules by a drop is sensitive to background gas far from the Knudsen regime. The insensitivity of the ''Potential OFF'' data to the carrier gas density indicates that the free molecule regime was well modeled.

IV. SLOPE OF THE CRITICAL SUPERSATURATION

From the above simulations it was possible to obtain the carrier gas effect factors $\xi(j,c)$ for 12 choices of the vapor, carrier gas, and temperature (see Table I). These choices are taken from the experimental works [3]. For each choice the factor $\xi(j,c)$ is obtained at $j = 20n$; $n = 1,\ldots,10$, and $c = 8n_1$ bars; $n_1 = 1,\ldots,5$, by 2×10^6 ''shots'' for each (j,c). (In the cases ''*ethanol*-He-$T = 363.4$ K'' and ''1-*propanol*–He–$T = 363.1$ K'' the range in j is extended to $n = 14$ and $n = 12$, respectively, since the critical sizes are large.) The carrier gas factors obtained are shown in Fig. 3. For each choice of the vapor and carrier gas, the effect is a bit stronger at lower temperature, and the corresponding surface lies just under the higher temperature surface. To integrate $\partial_c S_{\rm cr}(c)$, Eq. (4), numerically we used the factors $\xi(j,c)$ at $j \neq 20n$ or $c \neq 8n_1$ bars determined by linear interpolation. (As can be seen from Fig. 3, the slopes of ξ vs j and c are smooth enough; polynomial or rational interpolations did not change the final results appreciably.) For an initial value of $S_{\rm cr}$, we chose approximate values of $S_{\rm cr}$ (4 bars) from the experimental data [3] (see Table I). The classical critical sizes $j_{\rm cr}$ at these supersaturations are also given in Table I. Surface tension values are from [13]; the values of V are as in [3] (see references therein); the parameters ϵ_v, D_v, ϵ_c, and D_c are taken from [6].

Before proceeding further, we discuss the sensitivity of the evaporation rates $\gamma(j)$ to the carrier gas pressure. As suggested in [1] and confirmed by the present simulations, the carrier gas affects the impingement rates by small angle deflections (randomizations) of the vapor molecule trajectories near the drop. Such randomizations partially recover the Maxwell distribution for the velocities of molecules moving toward the drop. Roughly speaking, a molecule that would reach a drop only because of the drop's attraction, may miss the drop if disturbed by a carrier gas molecule. The same picture suggests that the effect on vapor molecules moving outward should be opposite: An ''evaporated'' vapor molecule with a trajectory bent back to the drop by the drop's attraction may be indeed evaporated if disturbed by a carrier gas molecule. The nonsymmetry of the situation is clear: it is easier for a molecule to be randomized away from the drop than toward the drop. Thus the carrier gas should increase the evaporation rates, and thus amplify the overall effect, which may be characterized, roughly, by the product

$$\prod_{l=1}^{j_{\rm cr}} \frac{\beta_e(l,c)\,\gamma(l+1,0)}{\beta_e(l,0)\,\gamma(l+1,c)} = \prod_{l=1}^{j_{\rm cr}} \xi(l,c)\,\frac{\gamma(l+1,0)}{\gamma(l+1,c)} \qquad (22)$$

TABLE I. The choices of the vapor (methanol, ethanol, and 1-propanol), the carrier gas (hydrogen and helium) and the temperatures T are taken from [3]. $S'_{\rm cr}$ is the critical supersaturation at 4 bars; $j'_{\rm cr}$ is the classical critical size at 4 bars; $\partial_c S^{\rm th}_{\rm cr}$ is the obtained here averaged slope of the critical supersaturation $S_{\rm cr}$ vs the carrier gas pressure c. $\partial_c S^{\rm exp}_{\rm cr}$ is the slope from the experimental work [3]. The values of A and B [see Eqs. (20) and (21)] are also shown.

Vapor	Carrier gas	T (K)	$S'_{\rm cr}$	$j'_{\rm cr}$	A	B	$\partial_c S^{\rm th}_{\rm cr}$ (bar^{-1})	$\partial_c S^{\rm exp}_{\rm cr}$ (bar^{-1})
Methanol	H_2	333.8	1.7	82	4988	1.26	2.9×10^{-3}	4.1×10^{-3}
		363.1	1.45	136	4586	1.27	2.4×10^{-3}	2.0×10^{-3}
	He	333.4	1.65	98	4994	1.26	1.6×10^{-3}	1.2×10^{-2}
		363.2	1.45	136	4585	1.27	1.2×10^{-3}	5.9×10^{-3}
Ethanol	H_2	329.8	1.95	88	3800	1.14	5.0×10^{-3}	1.25×10^{-2}
		364.0	1.6	125	3443	1.15	3.8×10^{-3}	5.6×10^{-3}
	He	329.1	1.85	114	3808	1.14	3.4×10^{-3}	2.82×10^{-2}
		363.4	1.5	197	3448	1.15	2.5×10^{-3}	1.18×10^{-2}
Propanol	H_2	334.6	2.4	75	5957	1.23	7.2×10^{-3}	2.02×10^{-2}
		362.5	1.9	105	5498	1.23	5.4×10^{-3}	1.14×10^{-2}
	He	334.2	2.25	91	5964	1.23	4.9×10^{-3}	4.72×10^{-2}
		363.1	1.75	157	5489	1.23	3.6×10^{-3}	2.00×10^{-2}

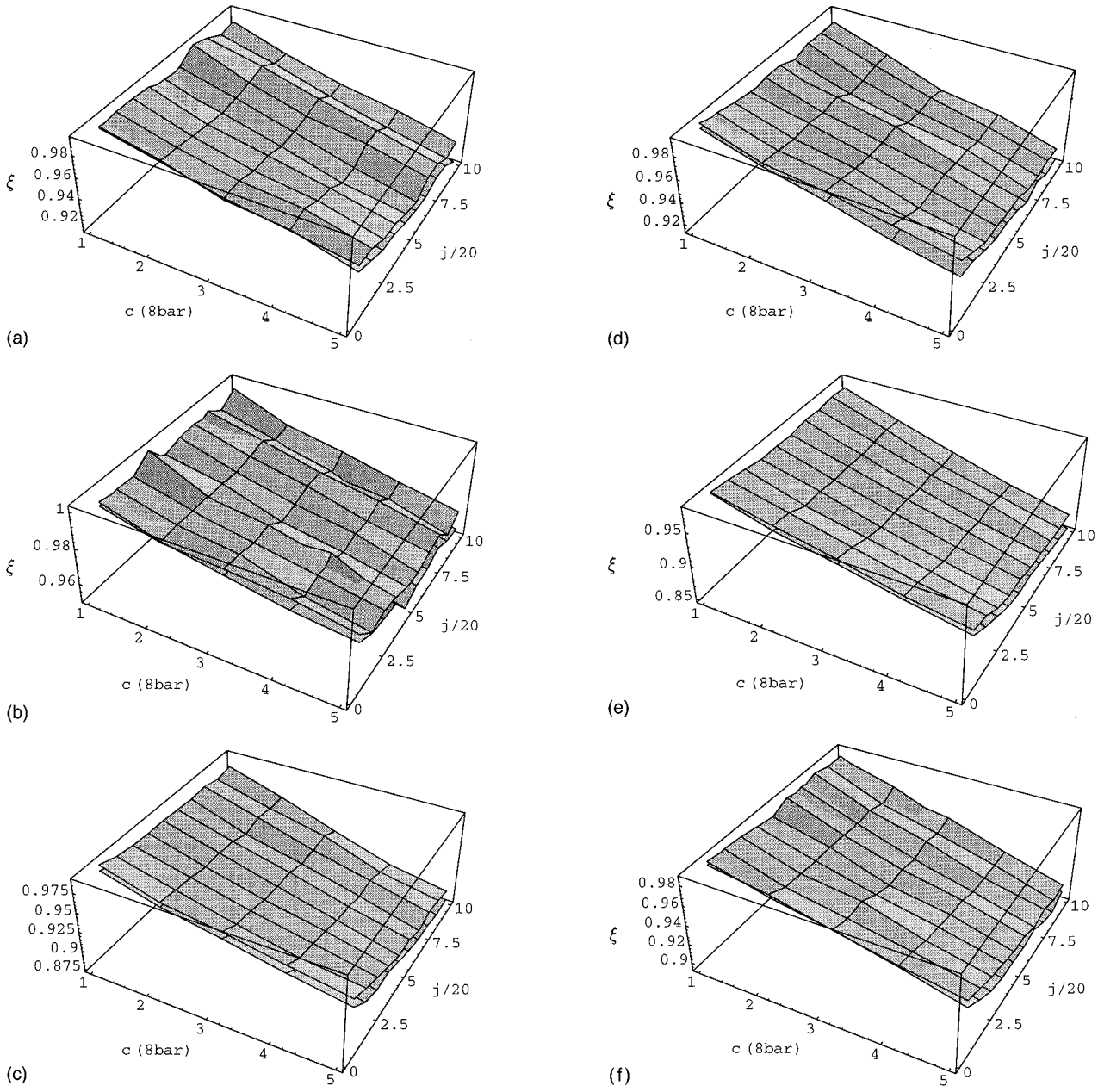

FIG. 3. The carrier gas factors ξ obtained from simulations. c is the carrier gas molecular density; j is the drop's size. Each figure corresponds to a choice of the vapor and carrier gas shown in Table I (and taken from [3]). (a) Methanol-H_2; (b) methanol-He; (c) ethanol-H_2; (d) ethanol-He; (e) 1-propanol–H_2; and (f) 1-propanol–He. The upper surface at each figure corresponds to a higher temperature (about 330 K, see Table I); the effect at lower temperature (about 360 K) is a little stronger and gives the surface right underneath, the edge of it shows up at each figure.

[see Eq. (1)] [1]. However, the same nonsymmetry suggests that the effect on the evaporation rates should be much weaker than the effect on the impingement rates. To illustrate our point, we have made ''inverse'' simulations. Namely, a vapor molecule is shot from the sphere of radius R_0+a, and considered to be successfully evaporated if it reaches the sphere of radius R_s. If the molecule reaches the sphere of radius R_0+a, it is counted as unsuccessfully evaporated. The velocity distribution of the molecules that are about to evaporate is not known (unless a special model of the drop is involved [14]), and for illustrative purposes we took the same distribution as in Eq. (14). Notice that we are interested in how the ratio of the number of the successfully evaporated molecules to the number of all shots, 2×10^6, depends on the carrier gas density. With increase of the carrier gas density the ratio increased, but this increase was several times weaker than the corresponding decrease of the impingement rate ξ. Thus $0<1-\gamma(l+1,0)/\gamma(l+1,c)\ll1-\xi(l,c)$. There is no theory to calculate $\gamma(l,0)/\gamma(l,c)$, but these arguments allow us to use Eqs. (2)–(4), based on the approximation $\gamma(j,c)=\gamma(j,0)\equiv\gamma(j)$.

The average slopes $\partial_c S_{\rm cr}$ obtained are presented in Table I. The extension mentioned above in the range of j in the cases ''*ethanol*-He-$T=363.4$ K'' and ''1-*propanol*–He–T

$=363.1$ K'' increased the values of $\partial_c S_{cr}$ 1.04 and 1.01 times, respectively. The slopes at different pressures c differ from the average by about 10%. For example, in the case ''*methanol*-H_2-$T=333.8$ K,'' we have the slopes, approximately, in units of 10^{-3} bars^{-1}, 2.8 at $c=8$ bars, 3.1 at $c=16$ bars, 2.7 at $c=24$ bars, and 2.9 at $T=32$ bars. In experiments [3] a linear dependence of S_{cr} on c was obtained, and the slopes $\partial_c S_{cr}$ from [3] are also given in Table I for comparison. The experimental values $\partial_c S_{cr}^{exp}$ are higher than the theoretical $\partial_c S_{cr}^{th}$ (except for the case ''*methanol*-H_2-$T=363.1$ K''). The discrepancy is larger at lower temperatures and with helium as a carrier gas, and reaches nearly one order of magnitude in several cases. Some trends are similar for $\partial_c S_{cr}^{exp}$ and $\partial_c S_{cr}^{th}$: The effect is stronger at lower temperature, and increases as the vapor is changed in the sequence ''methanol→ethanol→1-propanol.'' However, the experimental effect is stronger with helium as a carrier gas, while the calculated effect is stronger with hydrogen.

V. CONCLUSION

The well-known expression for the impingement rate of vapor molecules onto a surface (''surface area times average molecular velocity times the vapor density'') must be corrected for small objects such as nucleating droplets by taking into account the interaction between the object and the molecules. In the present work we have demonstrated through the simulation described in Sec. III, that this correction (enhancement) is sensitive to the background gas density. An increase of the carrier gas density decreases impingement rates and increases evaporation rates.

Thus the dense carrier gas makes the droplet less stable (increases the droplet's free energy). The effect is due to the interaction between the carrier gas and vapor molecules in an area around the droplet having about the droplet's size. The effect is not negligible only for very small droplets (see Fig. 2), and so the size of the area is far less than the vapor molecule mean free path and the effect cannot be obtained from bulk properties of the vapor-carrier gas mixture [15]. To obtain the resulting effect on the nucleation rate quantitatively, we used several approximations. We took the evaporation rates to be independent of the carrier gas density, arguing that they are, in any case, less sensitive to the carrier gas than the impingement rates. (We argued also that we underestimate the effect by using this approximation.) We used simple Lennard-Jones potentials for the interaction between molecules [6]. We also assumed unit sticking probabilities. (We probably underestimate the effect by using these two approximations, as well [1].) The effect calculated under such assumptions is comparable with the experimental data [3], which, to our knowledge, had not been previously explained by other mechanisms based on nucleation [15–17]. (However, the authors of [18] suggested an alternative qualitative explanation based on droplet growth. They argued that the reason for the observed [3,19–22] carrier gas effect in diffusion cloud chambers could be due to a slower growth of the drop to detectable size. As the carrier gas pressure increases the drop growth rate slows down and this may lead to undercounting of nucleation events.)

The calculated effect is strong: The ''small'' values of $\partial_c S_{cr}^{th}$, given in Table I, mean, in terms of the nucleation rate, increase of the rate by orders of magnitude with increase of the carrier gas pressure to 40 bars under fixed supersaturation. Notice that simple estimate can be made by using the fact that the carrier gas factors $\xi(j,c)$ do not depend strongly on j (see Fig. 3). We may substitute, roughly, $\partial_c A(j,c) \sim -A(j,c) j \partial_c \xi(j_{cr},c)/\xi(j_{cr},c)$ for Eq. (13) and $\partial_c S_{cr} \sim -S_{cr}\partial_c \xi(j_{cr},c)/\xi(j_{cr},c)$ for Eq. (4). Thus the effect of the carrier gas on S_{cr} should be of the same order as that on the carrier gas factor $\xi(j_{cr},c)$: about 10% per 40 bars in the cases considered. This is indeed the case, see Table I. If one measures the nucleation rate $J(c)$ under different carrier gas pressures and fixed supersaturation, the effect is, roughly, $J(c)/J(0) \sim \xi^{j_{cr}}(j_{cr},c)$ [see Eq. (2)]. In such measurements the effect can be seen only if j_{cr} is large enough [1]. Our results are given in terms of $\partial_c S$ at $J=$const rather than as $\partial_c J$ at $S=$const not only because the experimental results [3] were obtained in these terms, but also because an inaccuracy in $\partial_c S_{cr}(c)$ is related linearly to the inaccuracy in $\partial_c \xi(j,c)$, while an inaccuracy in J is certainly not.

ACKNOWLEDGMENTS

The authors thank Professor M. S. El-Shall, Professor S. P. Fisenko, and Dr. D. Kane for information about their works [18,22]. V.M.N. is indepted to Professor F. Boehm for the opportunity to visit Caltech. O.V.V. and H.R. acknowledge the support of the National Science Foundation under Grant No. CHE93-19519 and under a subcontract with Brookhaven National Laboratory supported by NASA through interagency agreement No. W-18429.

[1] O. V. Vasil'ev and H. Reiss, Phys. Rev. E **54**, 3950 (1996).
[2] O. V. Vasil'ev and H. Reiss, J. Chem. Phys. **105**, 2946 (1996).
[3] R. H. Heist, M. Janjua, and J. Ahmed, J. Phys. Chem. **98**, 4443 (1994); R. H. Heist, J. Ahmed, and M. Janjua, *ibid.* **99**, 375 (1995).
[4] J. L. Katz and H. Wiedersich, J. Colloid Interface Sci. **61**, 351 (1977); J. L. Katz and M. D. Donohue, Adv. Chem. Phys. **40**, 137 (1979).
[5] F. F. Abraham, *Homogeneous Nucleation Theory* (Academic, New York, 1974).
[6] R. C. Reid, J. M. Prausnitz, and B. E. Poling, *The Properties of Gases and Liquids*, 4th ed. (McGraw-Hill, New York, 1987).
[7] T. Kihara, *Intermolecular Forces* (Wiley, Chichester, 1978).
[8] G. F. Humber and U. M. Titulaer, J. Stat. Phys. **59**, 441 (1990); **63**, 203 (1991); M. E. Widder and U. M. Titulaer, Physica A **167**, 663 (1990); *Rarefied Gas Dynamics: Theory and Simulations* (American Institute of Aeronautics and Astronautics, Inc., Washington, D.C., 1992), p. 608; V. Chernyak, J. Aerosol Sci. **26**, 873 (1995).
[9] J. C. Barrett and B. Shizgal, in *Rarefied Gas Dynamics: Physical Phenomena* (American Institute of Aeronautics and Astronautics, Inc., Washington, D.C., 1989), p. 447.
[10] G. E. Kelly and J. V. Sengers, J. Chem. Phys. **57**, 1441 (1972); **61**, 2800 (1974).

[11] L. Monchick and H. Reiss, J. Chem. Phys. **22**, 831 (1954); J. C. Barrett and C. F. Clement, J. Aerosol Sci. **19**, 223 (1988).
[12] N. B. Vargaftik, *Handbook of Physical Properties of Liquids and Gases*, 2nd ed. (Hemisphere, Washington, D.C., 1975).
[13] J. J. Jasper, J. Phys. Chem. Ref. Data **1**, 841 (1972).
[14] B. Nowakowski and E. Ruckenstein, J. Chem. Phys. **94**, 1397 (1991); **94**, 8487 (1991); E. Ruckenstein and B. Nowakowski, Langmuir **7**, 1537 (1991).
[15] D. Kashchiev, J. Chem. Phys. **104**, 8671 (1996).
[16] I. J. Ford, in *Nucleation and Atmospheric Aerosols*, edited by N. Fukuta and P. E. Wagner (A. Deepak, Hampton, 1992), p. 39; J. Aerosol Sci. **23**, 447 (1992).
[17] J. C. Barrett, C. F. Clement, and I. J. Ford, J. Phys. A **26**, 529 (1993).
[18] D. Kane, S. P. Fisenko, and M. S. El-Shall (unpublished).
[19] A. Bertelsmann, R. Stuczynski, and R. H. Heist, J. Phys. Chem. **100**, 9762 (1996).
[20] V. N. Chukanov and B. A. Korobitsyn, Russ. J. Phys. Chem. **63**, 1085 (1989), and references therein.
[21] J. L. Katz, C.-H. Hung, and M. Krasnopoler, in *Atmospheric Aerosols and Nucleation*, edited by P. E. Wagner and G. Vali (Springer, Berlin, 1988); J. L. Katz, J. A. Fisk, and V. Chakarov, in *Nucleation and Atmospheric Aerosols*, edited by N. Fukuta and P. E. Wagner (A. Deepak, Hampton, 1992), p. 11.
[22] D. Kane and M. S. El-Shall, J. Chem. Phys. **105**, 7617 (1996).